Enhanced Confinement and Quasi-Single-Helicity Regimes Induced by Poloidal Current Drive

D. Terranova, A. Alfier, F. Bonomo, P. Franz, P. Innocente, and R. Pasqualotto

Consorzio RFX, Associazione Euratom-ENEA sulla Fusione-Corso Stati Uniti, 4, I-35127 Padova, Italy

(Received 24 April 2007; published 29 August 2007)

Enhanced confinement regimes with quasihelical symmetry are reproducibly obtained in the modified reversed field pinch eXperiment (RFX)-mod by reducing the level of internal chaos through the combination of a smooth magnetic boundary (through a virtual shell scheme) and the oscillating poloidal current drive technique. The plasma moves from a chaotic multiple helicity towards a quasi-single-helicity regime with a magnetic island showing high temperature and soft x-ray emissivity. The chaos reduction involves also the plasma outside the island allowing for a global enhanced confinement with an improvement up to 50%.

DOI: 10.1103/PhysRevLett.99.095001 PACS numbers: 52.55.Hc, 52.25.Fi, 52.25.Gj, 52.35.Py

Magnetic topology is an important aspect for understanding performances in magnetically confined plasmas. This is particularly true for the reversed field pinch (RFP) configuration where the system requires a substantial helical-like deformation of the equilibrium toroidal magnetic surfaces in order to sustain the mean magnetic field reversal [1], a process that is referred to as RFP dynamo. This deformation arises as saturated kink-tearing modes with poloidal periodicity $m = 1$ and toroidal periodicity $|n| \geq 2R/a$, (R and a are the major and minor radius of the experimental device). As a counterpart to this requirement, the equilibrium magnetic field is small with respect to the typical value in a tokamak, where a lower level of perturbation is present. To mitigate the detrimental effect of these perturbations, in the RFP community a significant effort is devoted to exploiting enhanced confinement regimes, i.e., configurations characterized by an overall reduced level of magnetic fluctuation or by favoring configurations that preserve good magnetic surfaces. Theoretically, the stability of a steady RFP in a helically symmetric state has been demonstrated [2] where a single mode with its harmonics provides all the necessary dynamo action preserving good magnetic surfaces. Experimentally, only quasi-single-helicity (QSH) states are observed [3–5], i.e., regimes where the magnetic fluctuation is dominated by a single mode, but also other harmonics are present, so that the improvement involves only a limited volume of the plasma and the overall level of chaos is not significantly reduced. However, an effective technique was devised at the MST experiment to reduce in a pulsed fashion the global level of fluctuations (the pulsed poloidal current drive, PPCD [6]) and successfully applied in all the RFP experiments [7–10]. The mechanism consists of varying the toroidal field at the edge so that a current profile modification is transiently induced in the plasma, concentrating the toroidal flux in the core [11]. This nonstationary condition quenches the natural dynamo process allowing for a reduction in the magnetic fluctuation level and an improvement both in temperature and energy confinement. To bypass the transient nature of the PPCD, an extension of the technique was devised in the RFX experiment: the oscillating poloidal current drive (OPCD) [12], where the toroidal field at the edge is modulated with a given frequency and amplitude, so that the PPCD is periodically repeated. In RFX the OPCD operations produce (averaging over the oscillation periods) the same enhanced regimes as the PPCD does, extending the improved performance over the whole duration of the external action. Furthermore over an OPCD oscillation cycle the average net input power is a negligible fraction ($< 0.5\%$) of the global input power [12]. In the RFX experiments a certain correlation was found between the OPCD action and the appearance of a QSH regime. The same experiments are now successfully applied to the modified RFX device (RFX-mod) [13] ($R = 2$ m and $a = 0.459$ m) with new results concerning this aspect: the induced reduction of the global magnetic fluctuation level is systematically associated with the formation of a QSH state, as well as to a global increase of the electron temperature and to a reduction of the electrons energy transport. As a result the configuration is moving towards the theoretically predicted single helicity state.

The experiments on RFX-mod took advantage of the improved magnetic boundary provided by the virtual shell system [14] (required since the passive shell time constant is $\tau_{\text{wall}} = \mu_0 \delta_s r_s / \eta_s \sim 100$ ms, where δ_s, r_s, and η_s are the shell thickness, minor radius and resistivity) and of the high flexibility of the power supply system providing the modulation (following an arbitrary waveform) of the toroidal magnetic field at the edge. This active system is coupled to a set of magnetic field pickup coils measuring the radial and toroidal field component by means of 4 arrays of 48 coils covering the whole torus.

The discharges considered here have a plasma current (I) between 0.5 and 1 MA and parameter I/N ($N = \pi a^2 \langle n_e \rangle$) between 4 and 8×10^{-14} A m.

The effect of the OPCD on the plasma and its magnetic spectrum is shown in Fig. 1 (thin line) compared to a reference discharge with spontaneous QSH phases (thick line). Both discharges are operaterd in the virtual shell scheme. The induced poloidal electric field at the edge

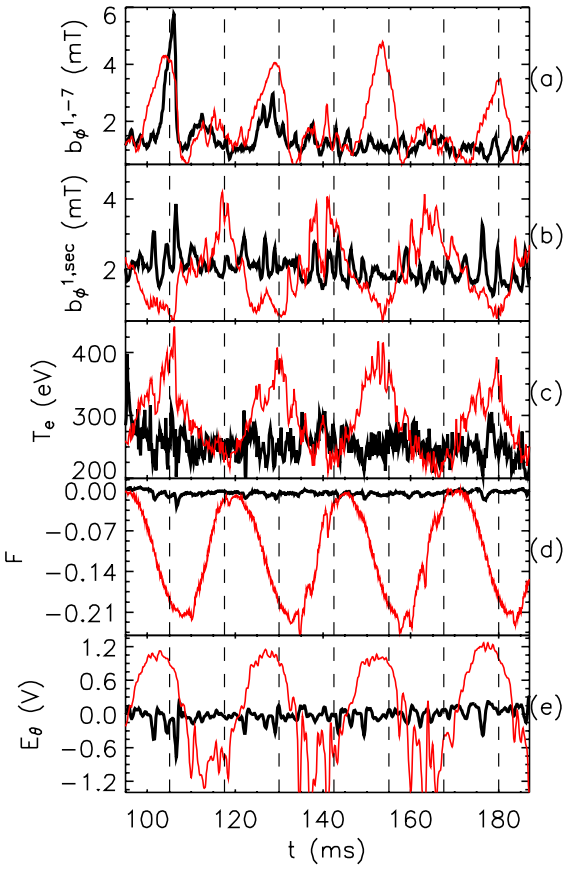

FIG. 1 (color online). Reference (thick line) and OPCD (thin line) shots. Time evolution of (a) dominant mode and (b) sum of secondary modes amplitudes, (c) T_e, (d) F and (e) poloidal electric field. $I \sim 700$ kA, $I/N \sim 4.5 \times 10^{-14}$ A m.

$E_\theta(a)$ is shown in panel (e). The codynamo phase is for $E_\theta(a) > 0$ and is characterized by a deeper reversal of the magnetic field [see the time evolution of the reversal parameter F ($= B_\phi(a)/\langle B_\phi \rangle$) in panel (d)]. During this phase the amplitude of the innermost resonant toroidal harmonic ($n = -7$) at the plasma edge increases [panel (a)], while that of secondary modes ($-15 \leq n \leq -8$) decreases significantly [panel (b)], resulting in a QSH spectrum. This is a first difference with respect to spontaneous QSH states where this reduction is not observed. As a result, in the phase of reduced internal chaos (when the OPCD oscillation is replacing the natural dynamo) one observes an increase in the electron temperature [panel (c)] measured by the double filter diagnostic [15].

The described change in the magnetic spectrum was already observed in the RFX device [12], even though the transition was not always induced by the external action, and an optimal period of oscillation was required to reach enhanced regimes. This is not the case on RFX-mod, where the OPCD almost always improves plasma performances and induces a QSH regime independently of the oscillation period. The combined effect on both T_e and the magnetic spectrum is presented in Fig. 2 where we show the probability distribution of the spectral spread

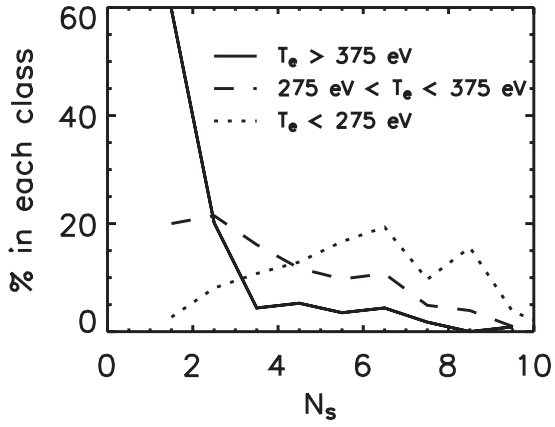

FIG. 2. Percentage distribution of the spectral spread number in three electron temperature classes.

number N_s [16] defined from the energy E_n of the $m = 1$ toroidal field harmonics as $N_s = [\sum_{n=-6}^{-20}(E_n/\sum_{n'}E_{n'})^2]^{-1}$. The discharges in the database were divided into three classes according to the maximum electron temperature reached during each OPCD: as the OPCD becomes more effective in terms of T_e increase, the transition to a QSH state becomes more frequent and stronger (smaller N_s). In particular, defining $N_s \leq 3.5$ for a QSH spectrum as in [4], more than 90% of the highest temperatures class is made of QSH discharges. Considering all together the database, it is clear that this technique is so far the most effective way of inducing a QSH state in RFX-mod.

The changes in the magnetic spectrum are not limited to the edge. Indeed by analyzing the radial profile of the eigenfunctions of the magnetic field (reconstructed in toroidal geometry from the external measurements [17]) one can determine the internal level of fluctuations and infer to what extent the OPCD is acting on the internal chaos. To this end in Fig. 3 we correlate the electron temperature with the internal amplitude of the radial magnetic field. In particular, we consider the maximum amplitude of each harmonic along the minor radius and extract two quantities

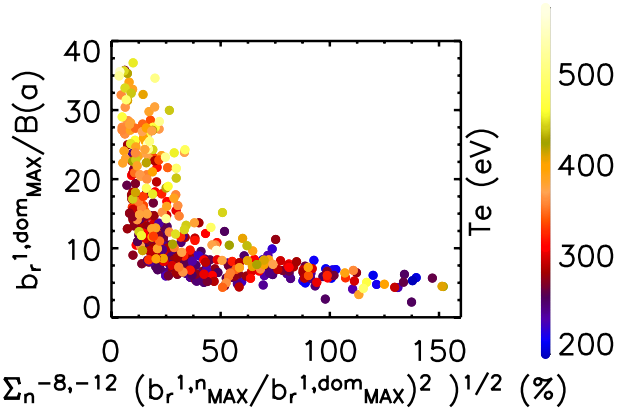

FIG. 3 (color online). T_e as a function of the normalized amplitude (the maximum value of the radial profile) of the dominant and the sum of secondary modes.

normalized to the magnetic field at the edge: the maximum of the dominant mode and the ratio between the total maximum of secondary modes (with n up to -12) and this value. From the figure it is clear that as the dominant mode increases its amplitude, the resulting electron temperature increases. However, best performances are obtained only if at the same time the amplitude of secondary modes is small with respect to the leading mode. The reduced level of chaos, reached in the region where secondary modes are resonant, allows for the formation of a clear structure in the SXR emissivity distribution visible in the tomographic reconstruction [see Fig. 4(a) compared to (b)] obtained from 78 lines of sight covering the plasma cross section [18]. This structure is well correlated with the magnetic QSH that is observed and is also representative of a thermal structure as will be shown in the following parts.

It is important to underline that secondary modes do not play a marginal role at all since their reduction seems to be the important ingredient to reach enhanced confinement regimes. This is shown by the electron temperature profile obtained with a multichord double-filter diagnostic [19]. In Fig. 4 we show the used chords on top of the tomographic reconstructions, and in Fig. 5 the corresponding profiles obtained for a MH (empty circles) and a QSH (full circles) phase of an OPCD cycle. The T_e increase involves the core ($0 < p < 0.16$ m), where the SXR structure is formed (providing a first indication that this is indeed a thermal structure), but also the plasma surrounding the island ($p > 0.18$ m), so that there is a global improvement of confinement in the plasma column.

Indeed this is the difference between spontaneous QSH regimes and those induced by OPCD: the transport within the island itself in the two cases is similar; however, the reduction in the chaos from secondary modes [see Fig. 1 panel (b)] induced by the OPCD in the volume close to (but outside of) the island allows for the formation of an island with a smaller dominant mode (with respect to a spontaneous QSH) and higher T_e. It is the overall reduced level of fluctuation due to the OPCD that produces the enhanced confinement. This is an important result since the volume defined by the island itself can be small compared to the total volume of the plasma, while in the OPCD the whole plasma enters an enhanced confinement regime, so that the OPCD is not simply a way of stirring the growth of a single mode, it also reduced transport outside the structure allowing record temperatures for RFX-mod above 700 eV.

The improvement observed in the codynamo phase, is typically reduced during the counterdynamo phase so that the system undergoes a cycle following the external oscillation. However, there are some cases in which the thermal structure survives this latter phase though it is reduced in amplitude. This again happens when secondary modes remain small. In some other cases, on the other hand, the plasma core is characterized by a high emissivity with a symmetric profile that in the following OPCD cycle changes again into an asymmetric structure.

The topological changes observed by magnetic and tomographic reconstructions are also visible in the temperature profile measured with the Thomson scattering diagnostic, providing the final proof that one is actually observing thermal structures. The diagnostic is capable of working at 50 Hz, measuring T_e at 84 spatial points along the plasma cross section [20]. In Fig. 6 we show two typical examples of the temperature profile obtained in OPCD discharges at the maximum of the electron temperature. Two features are significant to observe compared to the reference profile (empty circles): on the one hand the asymmetric peak in the profile (dark red circles) is well correlated with the dominant mode induced by the external action; on the other hand in some cases this peak becomes nearly symmetric (light green circles) and involves a larger fraction of the plasma cross section.

In standard discharges of RFX-mod, T_e profiles are generally flat in the core, indicating a fast energy transport in this region. On the other hand, the OPCD produces QSH states with a thermal island in this same region so that the energy transport in the core is reduced. In particular, in the case of asymmetric profiles the ∇T_e produced by the

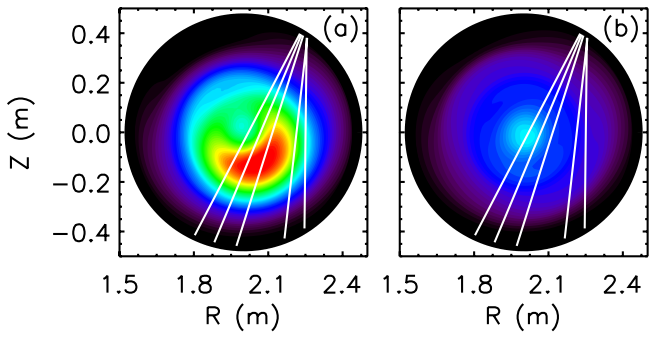

FIG. 4 (color online). SXR tomographic reconstruction in the QSH (a) and MH (b) phase of an OPCD ($I_p = 960$ kA, $I/N = 7.9 \times 10^{-14}$ A m). White lines are the multichord double-filter diagnostic.

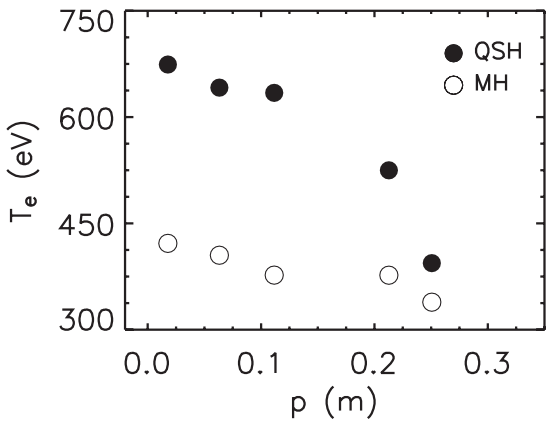

FIG. 5. T_e as a function of the impact parameter of the chords of the double-filter diagnostic. Full circles: at maximum T_e for the shot of Fig. 4 (QSH). Empty circles: at the minimum of T_e during the OPCD cycle (MH).

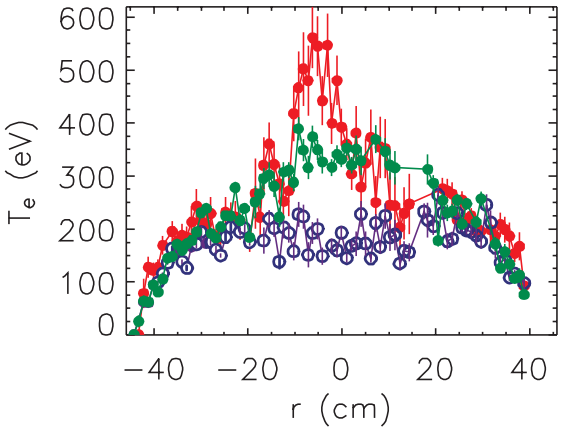

FIG. 6 (color online). T_e profiles. Empty circles: standard discharge (similar to the minimum T_e in an OPCD cycle). Full circles, light green: at maximum T_e (nearly symmetric profile). Dark red: at maximum T_e (asymmetric profile). $I = 610$ kA and $I/N = 3.3$–3.7×10^{-14} A m.

thermal structure is similar to or even larger than that at the edge of the plasma. Given the different plasma characteristics (in terms of N_e and T_e) at the edge and the core, the energy transport at the island edge is significantly smaller than at the plasma edge. We quantified the improvement with a simple power balance calculation (using a 1D approximation) determining the value of χ in the region where ∇T_e is strong (i.e., plasma edge and island edge). Considering the profiles of Fig. 6, one finds $\chi \sim 100$ m^2 s in the region with $|r| > 35$ cm and a value >500 m^2 s in the core (empty circles, flat profile). On the other hand, in the cases where an internal ($|r| < 20$ cm) ∇T_e is developed one finds that a nearly symmetric profile (light green circles) gives $\chi \sim 80$ m^2 s—a value close to the edge one—and an asymmetric profile (dark red circles) gives $\chi \sim 10$ m^2 s, an indication of a significant improvement of local confinement.

The improved performance due to the OPCD is also present in terms of global confinement time. A precise calculation is not easy when an asymmetric thermal structure is present, since it would require a two dimensional modeling. However, the externally induced QSH typically involves a mode resonant very close to the magnetic axis so that one can determine with a good approximation the confinement time by splitting in two the cross section of the plasma: one side includes the structure and the other does not. For this calculation the electron density profile was measured with a two-color, 8-chord interferometer [21], that, differently from T_e measurements, never shows an asymmetric profile. Considering the discharges of Fig. 6, we obtain an energy confinement time (τ_E) equal to 0.87 ms for the reference discharge (flat blue profile), a value of $\tau_E = 1.4$ ms for the nearly symmetric profile (green line), and $\tau_E = 1.3$ for the asymmetric profile (red line). These values, compared to the OPCD oscillation period, clearly show that the effect is significant and beneficial for the whole plasma.

In summary, we have shown that the OPCD technique coupled to an improved magnetic boundary—obtained in the virtual shell scheme—is an effective way for enhancing plasma performances both in terms of temperature and confinement. The improved state is characterized by the transition from a chaotic multiple helicity towards a quasi-single-helicity regime where an internal magnetic island is associated to high temperature and SXR emissivity region. The global improvement (up to 50%) is due to the combination of a magnetic island surrounded by a region (involving a large section of the plasma) of reduced chaos due to the induced reduction of secondary modes. The transition from a chaotic to an ordered magnetic configuration is triggered systematically and provides a significant experimental evidence to theoretical and numerical effort that has been put into understanding its spontaneous [22,23] and induced [24] occurrence. Besides the RFP, this is an important topic also for the tokamak and stellarator community since it concerns the effect of magnetic islands on transport phenomena.

This work was supported by the European Communities under the contract of Association between Euratom/ENEA.

[1] S. Ortolani and D. D. Schnack, *Magnetohydrodynamics of Plasma Relaxation* (World Scientific, Singapore, 1993).
[2] S. Cappello and D. F. Escande, Phys. Rev. Lett. **85**, 3838 (2000).
[3] D. F. Escande *et al.*, Phys. Rev. Lett. **85**, 1662 (2000).
[4] T. Bolzonella and D. Terranova, Plasma Phys. Controlled Fusion **44**, 2569 (2002).
[5] L. Marrelli *et al.*, Phys. Plasmas **9**, 2868 (2002).
[6] J. S. Sarff *et al.*, Phys. Rev. Lett. **72**, 3670 (1994).
[7] R. Bartiromo *et al.*, Phys. Rev. Lett. **82**, 1462 (1999).
[8] B. E. Chapman *et al.*, Phys. Plasmas **9**, 2061 (2002).
[9] Y. Yagi *et al.*, Phys. Plasmas **10**, 2925 (2003).
[10] M. Cecconello *et al.*, Plasma Phys. Controlled Fusion **46**, 145 (2004).
[11] M. E. Puiatti *et al.*, Nucl. Fusion **43**, 1057 (2003).
[12] T. Bolzonella *et al.*, Phys. Rev. Lett. **87**, 195001 (2001).
[13] P. Sonato *et al.*, Fusion Eng. Des. **66**, 161 (2003).
[14] S. Martini *et al.*, in *Proceedings of the 21st IAEA Fusion Energy Conference, Chengdu, China, 16–21 October, 2006*, Vol. EX/7-3 (unpublished).
[15] A. Murari *et al.*, Rev. Sci. Instrum. **70**, 581 (1999).
[16] Y. L. Ho *et al.*, Phys. Plasmas **2**, 3407 (1995).
[17] P. Zanca and D. Terranova, Plasma Phys. Controlled Fusion **46**, 1115 (2004).
[18] P. Franz, Nucl. Fusion **41**, 695 (2001).
[19] F. Bonomo *et al.*, Rev. Sci. Instrum. **77**, 10F313 (2006).
[20] A. Alfier and R. Pasqualotto, Rev. Sci. Instrum. **78**, 013505 (2007).
[21] P. Innocente *et al.*, Rev. Sci. Instrum. **68**, 694 (1997).
[22] S. Cappello, Plasma Phys. Controlled Fusion **46**, B313 (2004).
[23] S. Cappello *et al.*, Phys. Plasmas **13**, 056102 (2006).
[24] F. Ebrahimi *et al.*, Phys. Plasmas **11**, 2014 (2004).